Supplementary Material for "Direct Photolysis of α-Pinene Ozonolysis Secondary Organic Aerosol: Effect on Particle Mass and Peroxide Content"

Scott A. Epstein, Sandra L. Blair, Sergey A. Nizkorodov*
* nizkorod@uci.edu Ph: (949) 824-1262 Fax: (949) 824-8571
Department of Chemistry, University of California, Irvine

Contents

9 Pages, 11 Figures

Ozone Removal by Denuders

In order to test the efficiency of denuders, the ozone and VOC concentrations were recorded before and after the denuder train. The ozone concentration was reduced by at least a factor of 400 (Fig. S1). The effect of denuders on reducing VOC is shown in Fig. S2; the VOC levels were reduced by up an order of magnitude.

Figure S1: Ozone signal as measured before and after the denuder train. The monitor was moved between 16 and 30 minutes. The charcoal denuders remove ozone such that resulting concentrations are below detection limits. The denuder efficiency for ozone is greater than 400.

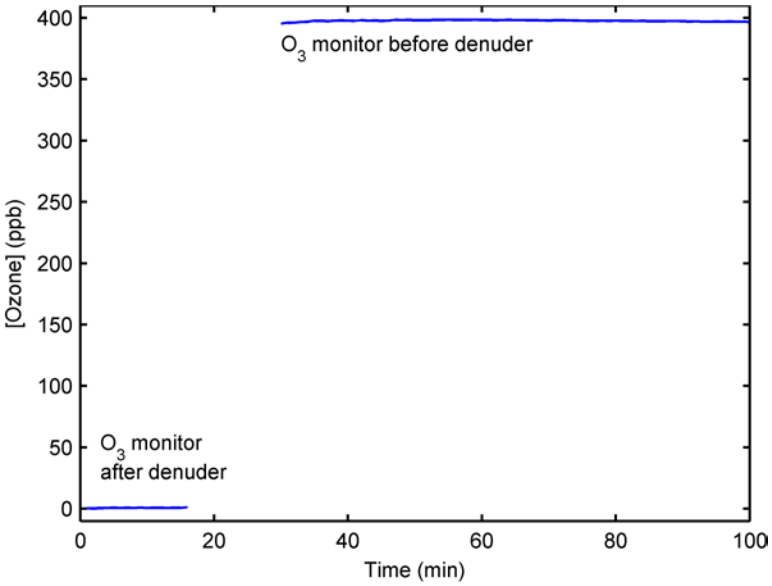

Changes in VOC Content through Denuder and upon Irradiation

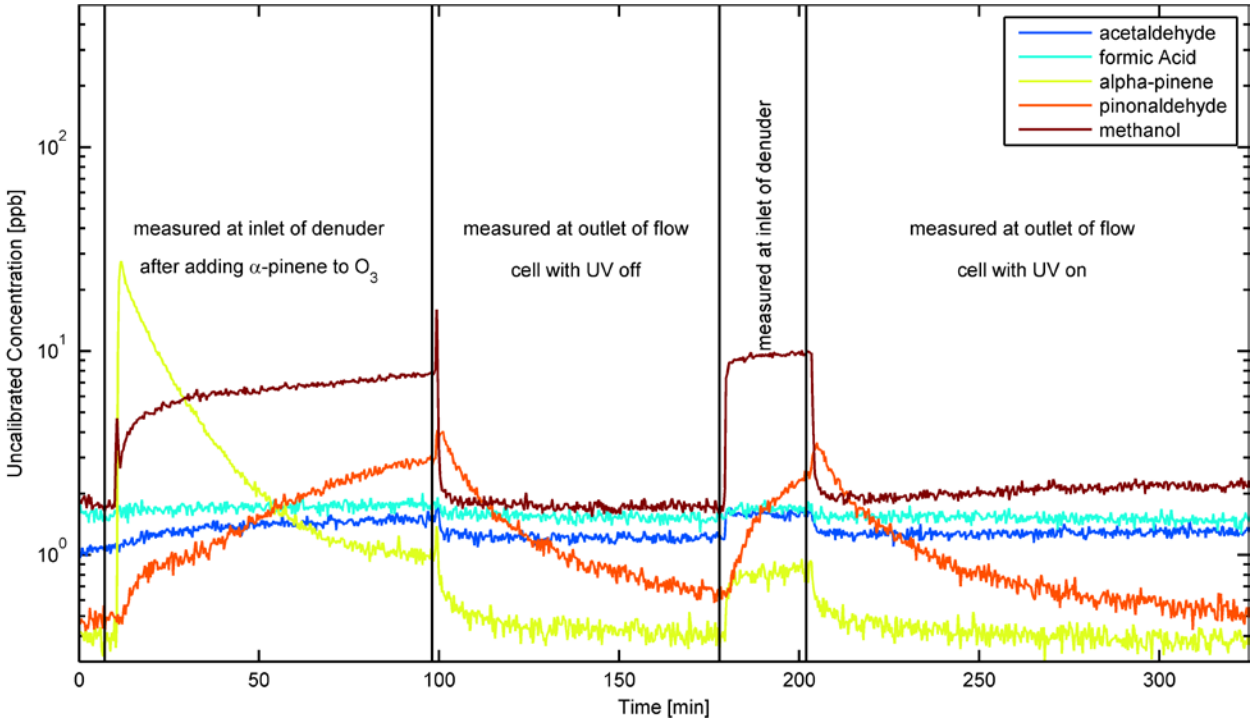

Figure S2: PTR-ToF-MS data showing the removal of VOCs after passing through the denuder and the generation of methanol upon photolysis of α–pinene ozonolysis SOA. The decay of α–pinene upon reaction with ozone is also evident. Pinonaldehyde is slow to respond due to its propensity to absorb to PTR-ToF-MS transfer line tubing.

Potential Effects of Temperature on SOA

To confirm that SOA photolysis, and not particle heating, is responsible for changes in particle size and chemical composition, we measured the temperature of air leaving the quartz UV-transparent flow cell and the foil-wrapped borosilicate flow cell at the lowest experimental flow rate. The temperature of the air in both the dark and light flow cell each rose slightly (~3^{o}C over an hour) at the same rate, confirming that temperature effects are properly accounted for with the "dark" flow cell. To ensure that heating was not changing particle composition, we intentionally heated the quartz flow cell by 4.4^{o}C and tracked particle composition with the ToF-AMS. We did not observe significant changes in chemical composition upon heating (See Fig. S3). In addition, heat-transfer calculations of particle heating by the UV-lamp confirm that the UV-light intensity is not strong enough to heat the particles beyond the temperature of the bulk gas (see below).

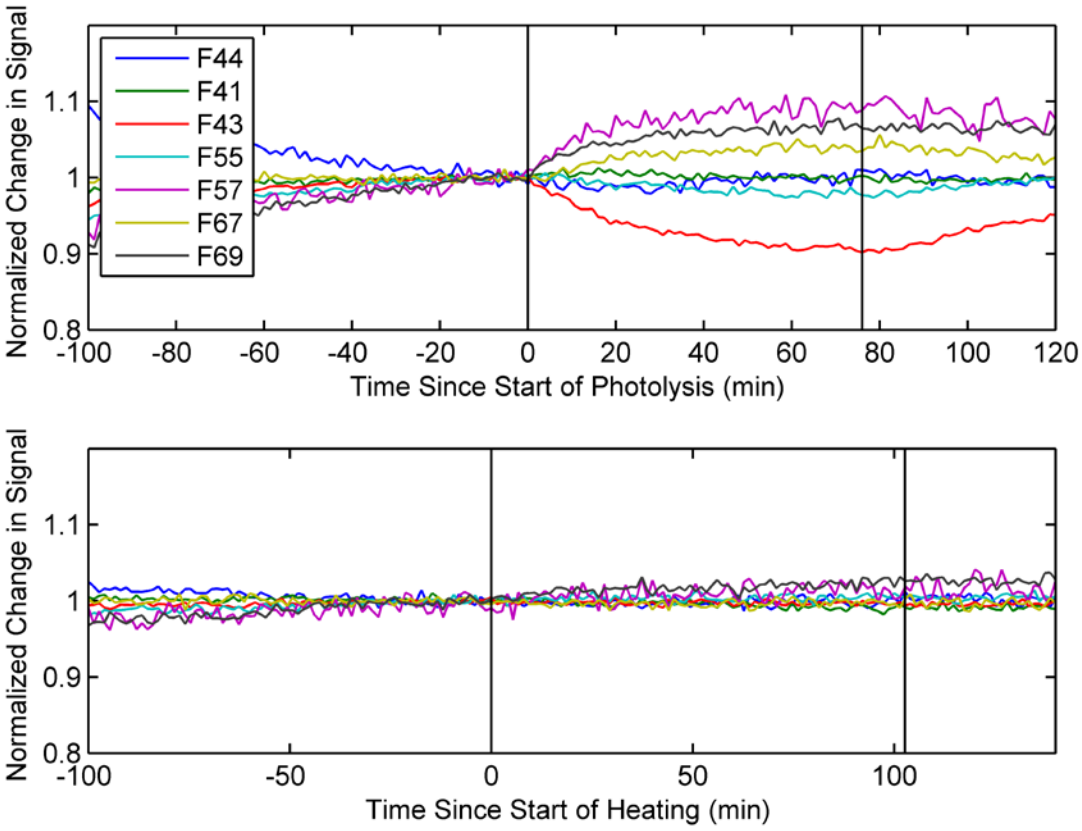

Figure S3: The normalized change in signal for seven key unit-masses as measured by the HR-AMS. The upper pane details changes in these key masses when the SOA is photolyzed (time = 0) and the lamps are turned off (indicated by the second vertical black line). The lower pane details changes when the SOA is heated by 4.4^{o}C inside the flow cell. The second vertical black line indicates when the heat source was removed.

Quantification of UV-light Intensity in the Flow Cell

In order to determine the intensity of the UV-lamps, we photolyzed isopropyl nitrite (IPN), a compound with a known photolysis quantum yield.[1] We mixed 14 ppm of IPN with 227 ppm of cyclohexane to serve as a hydroxyl radical scavenger in the smog chamber. We then pumped this mixture through the quartz flow cell and measured the relative concentration of isopropyl nitrite with the PTR-ToF-MS.

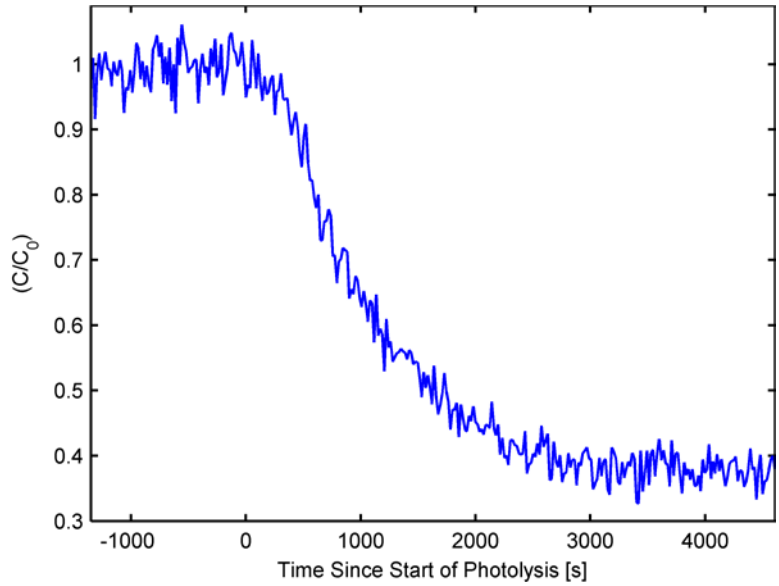

Figure S4: Change in relative concentration of isopropyl nitrite after the UV-lamps were turned on (at t=0) measured with the PTR-ToF-MS. For this experiment, the residence time in the flow cell was one hour. The flux is determined from comparison of the steady-state values of IPN before and after photolysis, as described below.

UV lamps were turned on until a steady-state concentration of IPN was established. A mass balance on IPN concentration at steady state yields the following relationship for the loss of IPN along the length of the flow cell in a plug-flow limit:

$$\frac{dC_{IPN}}{dV} = -\frac{J_{IPN}C_{IPN}}{Q} \qquad \text{(Eq. S1)}$$

C_{IPN} is the molar concentration of IPN [*mol/volume*], V is the incremental reaction volume, J_{IPN} is the first-order photolysis rate constant [$time^{-1}$], and Q is the flow rate of IPN through the flow cell [*volume/time*]. Integration yields the following equation relating the ratio of the initial and final IPN concentration to the residence time, τ, and the photolysis rate constant:

$$ln\left(\frac{C_{IPN}^{0}}{C_{IPN}^{F}}\right) = J_{IPN}\tau \qquad \text{(Eq. S2)}$$

It is also possible to derive a different equation that treats the flow cell as a continuously-stirred-tank-reactor. However, the plug-flow working equation appears to better capture the behavior of the flow cell as it leads to more reproducible UV-light intensities measured at different residence times. With the average quantum yield of IPN (<Φ> [*molecule/photon*]), the absorption cross section of IPN (σ(λ) [$distance^2$ $molecule^{-1}$]), and the unscaled dimensionless

wavelength dependence of UV-light inside the flow cell, $U(\lambda)$ (measured with a spectrometer), we could calculate the effective spectral flux density of photons inside the flow cell as a function of wavelength, $F_{lamp}(\lambda)$ [*photons* s^{-1} *volume*$^{-1}$]:

$$F_{lamp}(\lambda) = \frac{U(\lambda)\cdot J_{IPN}}{\langle\Phi\rangle \int U(\lambda)\cdot\sigma(\lambda)\cdot d\lambda} \qquad \text{(Eq. S3)}$$

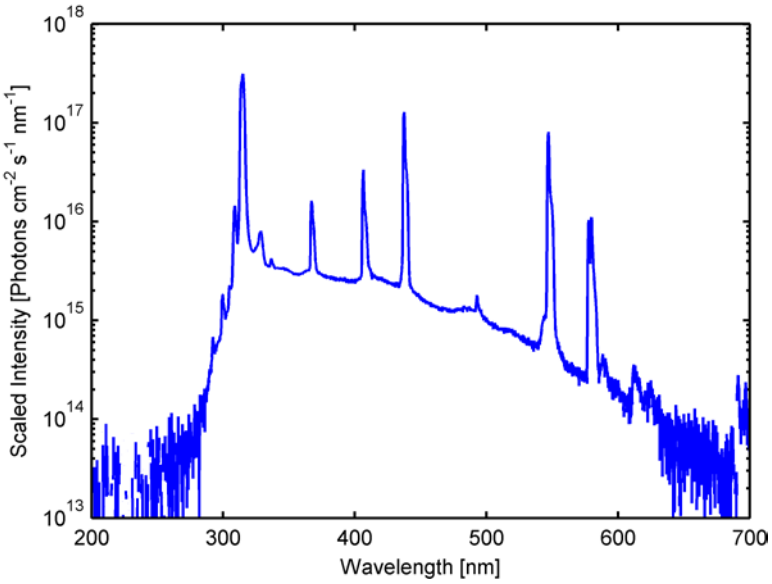

Figure S5: Wavelength dependence of the UV-light used to photolyze the aerosol. The intensities are scaled by using the isopropyl nitrite actinometer to quantify the power of the lamps. The majority of the intensity is carried by the 312 nm line. The amount of radiation from wavelengths below 300 nm is negligible (note the logarithmic scale). Radiation above 350 nm does not significantly contribute to photolysis because of the low absorption cross sections of SOA at these wavelengths.

$F_{lamp}(\lambda)$ shown in Fig. S5 represents the number of photons crossing a unit area per time per wavelength interval. Ideally, the quantum yield of IPN photolysis would also be a function of wavelength. However, wavelength-dependent measurements of quantum yield require several different monochromatic light sources and were not available in the literature. Assuming that the quantum yield of IPN is independent of wavelength within the UV region may lead to a slight bias in the estimated atmospheric photolysis lifetime. We define the unitless ratio of lamp intensity to the intensity of solar radiation, E, as:

$$E = \frac{\int F_{lamp}(\lambda)\cdot\sigma_{SOA}(\lambda)\cdot d\lambda}{\int F_A(\lambda)\cdot\sigma_{SOA}(\lambda)\cdot d\lambda} \qquad \text{(Eq. S4)}$$

where $F_A(\lambda)$ [*photons* s^{-1} *volume*$^{-1}$] is the actinic flux at the 24-hour-averaged solar zenith angle in Los Angeles on the summer solstice predicted by the NCAR/ACD Tropospheric Ultraviolet and Visible Radiation Model[2] with a surface albedo of 0.15. The unitless ratio, E, is used to convert laboratory-determined photolysis lifetimes to tropospheric lifetimes. A typical value for our experiments was E = 414 ± 30 when calculated for the 24-hour average solar flux in Los Angeles. The absorption spectrum of α-pinene ozonolysis SOA was obtained from UV-vis absorption measurements of SOA from Ali et al.[3] The absorption cross section of IPN, digitized from Ludwig and McMillan,[1] and the molar extinction coefficients of α-pinene ozonolysis SOA are shown in Fig. S6. Since absorption cross sections appear as a ratio as in Eq. S4, and its units

cancel out, molar extinction coefficients *ε(λ)* [volume mole^{-1} distance $^{-1}$] or even measured SOA absorbance can be used in this equation. However, for the sake of consistency, we converted all units to those of base-e absorption cross sections, typically used in gas-phase measurements. We used an effective molecular weight of 300 gm mol^{-1} for the SOA molecules in this conversion.

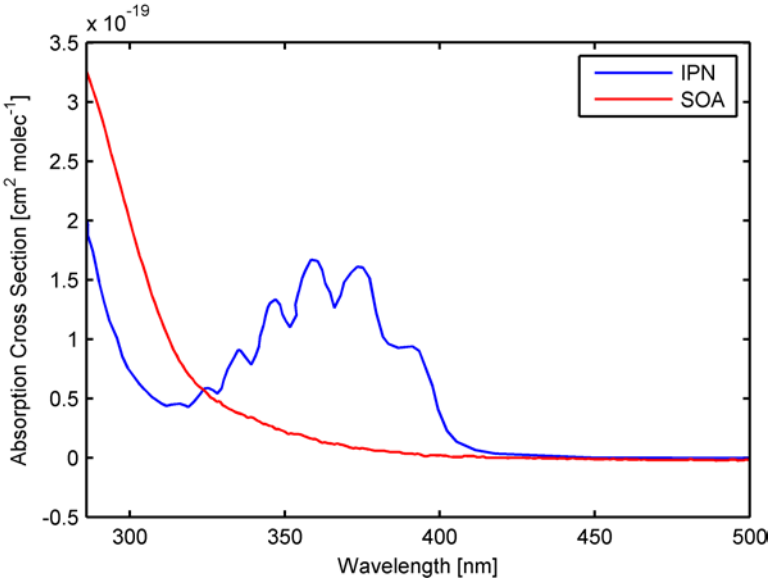

Figure S6: Absorption cross section of IPN and the molar extinction coefficient of α-pinene ozonolysis SOA.

The product of the absorption cross section of IPN and the effective spectral flux density of light entering the flow tube as a function of wavelength is shown graphically in Fig. S7. This "action spectrum" shows which wavelengths contribute the most to photochemistry (these values appear in the numerator and denominator of Eq. S4). The major wavelength contributing to photochemistry in our measurements is 312 nm. Figure S8 shows a similar action spectrum for the SOA photolysis, which is also dominated by the 312 nm wavelength.

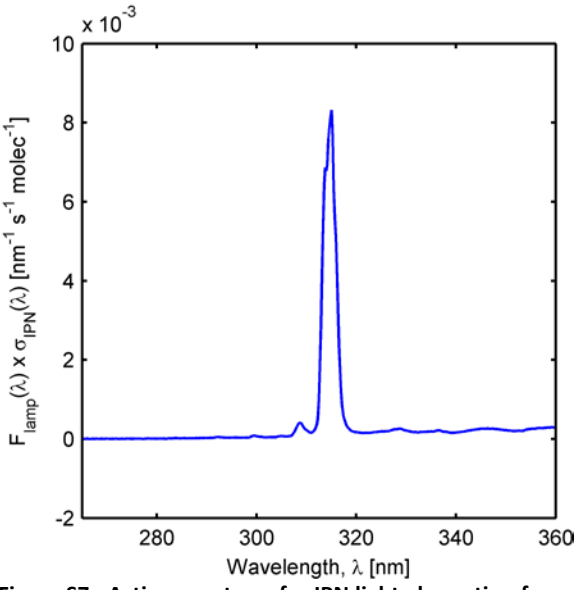

Figure S7: Action spectrum for IPN light absorption from the UV-lamp

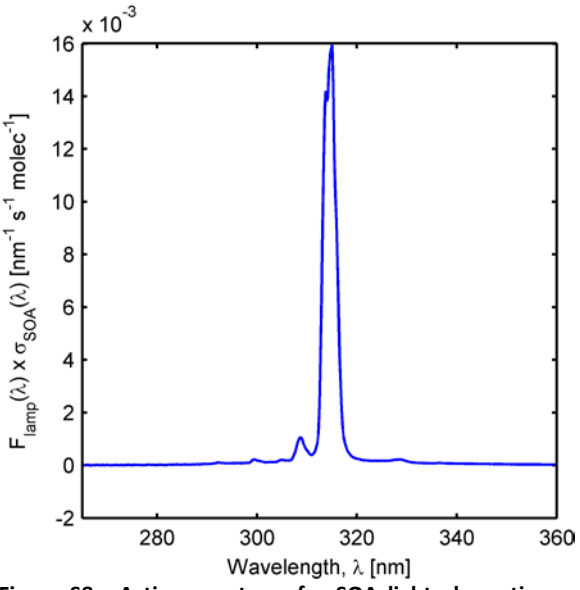

Figure S8: Action spectrum for SOA light absorption from the UV-lamp.

The action spectrum for the SOA light absorption from sunlight is shown in Fig. S9. Because the solar spectrum is more uniform than that of the UV lamp, a broader range of wavelengths, from 300 to 380 nm contribute to SOA photolysis.

Figure S9: Action spectrum for SOA light absorption from sunlight at a solar zenith angle of 65^{o}

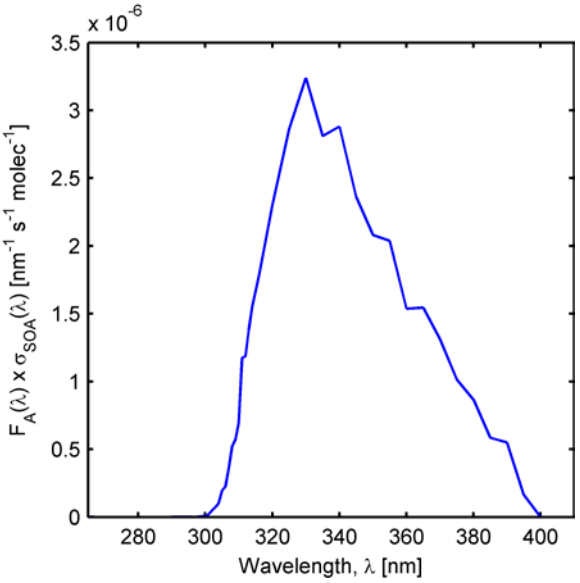

Negligible Overheating of Aerosol Particles

At steady-state the heat supplied to the particles from the UV lamps is removed by convection and conduction to the bath gas. We assume that the particle temperature is uniform and conduction is negligible. Assuming that conduction does not affect the particle temperature provides an upper estimate of the particle temperature at equilibrium. Therefore,

$$P_{h\nu}V_p\left(\frac{N_A\rho}{M_w}\right) = hA\left(T_p - T_{bath}\right) \qquad \text{(Eq. S5)}$$

where $P_{h\nu}$ is the power per molecule of the lamp, V_p is the volume of the particle, N_A is Avogadro's number, ρ is the particle density, M_w is the average molecular weight of the particle, h is the heat transfer coefficient, A is the particle surface area, T_p is the temperature of the particle, and T_{bath} is the temperature of the "bath" gas carrying the aerosol. The power of the lamp is derived from the isopropyl nitrite actinometer data and the absorption cross section of α–pinene SOA.

$$P_{h\nu} = \int \frac{h_p c}{\lambda}\sigma(\lambda)F_{lamp}(\lambda)d\lambda \qquad \text{(Eq. S6)}$$

h_p is Plank's constant, c is the speed of light, λ represents wavelength, $\sigma(\lambda)$ is the absorption cross section of α-pinene SOA, and $F_{lamp}(\lambda)$ is the flux of photons entering the flow cell as a function of wavelength. Equation S5 can be re-arranged to the following form:

$$T_p = \frac{1}{6}\frac{P_{h\nu}D}{h}\left(\frac{N_A\rho}{M_w}\right) + T_{bath} \qquad \text{(Eq. S7)}$$

where *D* is the particle diameter. The temperature enhancement resulting from the absorption of UV and the resulting convection to the bath gas, Δ*T*, can be written as:

$$\Delta T = \frac{1}{6}\frac{P_{h\nu}D}{h}\left(\frac{N_A\rho}{M_w}\right) \quad \text{(Eq. S8)}$$

For a spherical particle, the heat transfer coefficient *h* can be obtained from the following empirical relationships:

$$Nu = 2 + \frac{0.589 \cdot Ra^{1/4}}{\left[1+\left(\frac{0.469}{Pr}\right)^{9/16}\right]^{4/9}} \quad \text{(Eq. S9)}$$

$$Gr = \frac{D^3\rho^3 g\Delta T\beta}{\mu^2} \quad \text{(Eq. S10)}$$

$$Nu = \frac{hD}{k} \quad \text{(Eq. S11)}$$

$$Pr = \frac{\mu C_P}{k} \quad \text{(Eq. S12)}$$

$$Ra = Gr \cdot Pr \quad \text{(Eq. S13)}$$

where *Nu*, *Gr*, *Pr*, and *Ra* are dimensionless numbers, *g* is the gravitational constant, *k* is the thermal conductivity of air, C_p is the heat capacity of air, β is the coefficient of volume expansion of air, and μ is the viscosity of air. For a 100 nm particle with a density of 1.5 g cm^{-3}, the temperature enhancement is less than 2 x 10^{-6} K indicating that evaporation resulting from particle heating is negligible.

Average O:C Ratio of SOA in Case Studies A, B, and C

Figure S10: Average oxygen to carbon ratio (O:C) of the SOA from the ToF-AMS before and after photolysis for all three case studies. The change in the O:C ratio is approximately the same in all cases. This observation implies that photochemistry of gas-phase compounds (which are present in case B and reduced substantially in case A) has an insignificant effect on particle composition compared to the condensed-phase photochemical processes occurring in the particles.

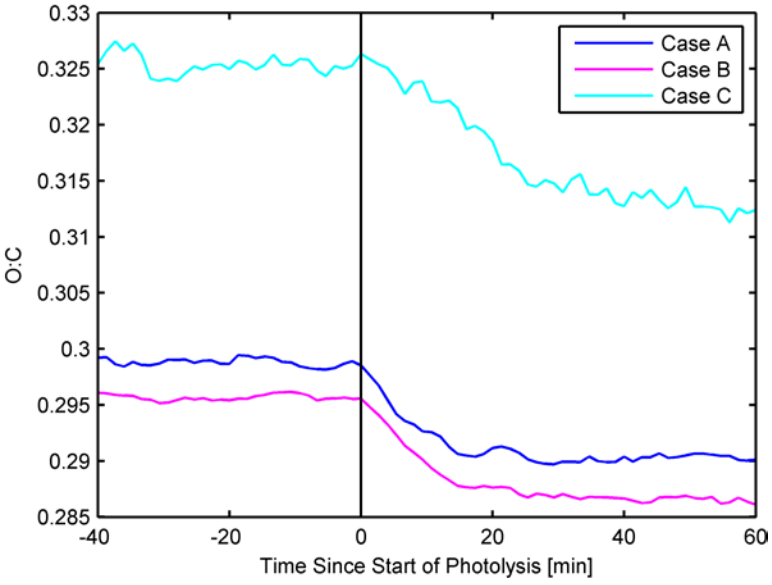

Aerosol Peroxide Lifetime in Los Angeles Throughout the Year

Figure S11: Aerosol peroxide lifetime in the atmosphere in Los Angeles, CA (34° latitude) as a function of month. The increase in the lifetime in winter months is due to the drastic reduction in the 24-hour average solar zenith angle.

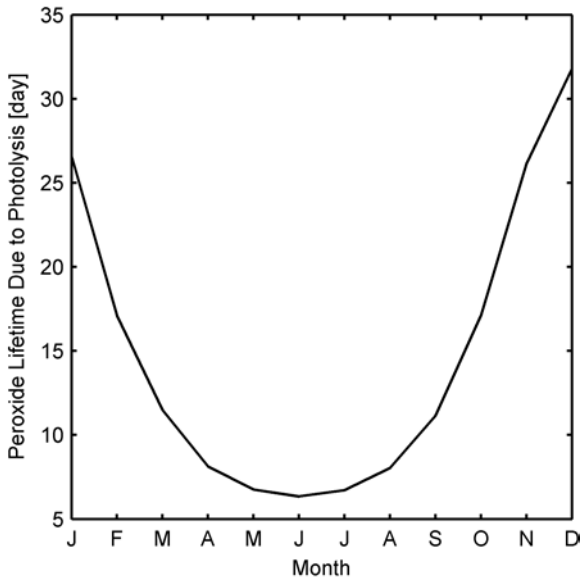

References

1. Ludwig, B. E.; McMillan, G. R., Primary quantum yields in photodissociation of isopropyl nitrite. *Journal of the American Chemical Society* 1969, *91*, (5), 1085-1088.
2. Madronich, S. *TUV: Tropospheric Ultraviolet and Visible Radiation Model, NCAR/ACD*, available at: http://cprm.acd.ucar.edu/Models/TUV/index.shtml, last access: October 2013.
3. Ali, N.; Saiduddin, M.; Wu, M.; Lee, H. J.; Romonosky, D. E.; Nizkorodov, S. A., Wavelength-Dependent Absorption Coefficients and Photolysis Rates of Model Anthropogenic and Biogenic Secondary Organic Aerosols. *In preparation* 2014.